Outline:

1. **Background Introduction**
2. **Fundamentals of Integrated Photonics**
3. **Derivation of Optical Waveguide Modes**
4. **Coupling Between Waveguides**
5. **Simulation Tools**
6. **Tasks**

1. Background Introduction

1.1 What is integrated photonics?

Integrated photonics is a field that enables **the manipulation of light on a chip**, offering a scalable and compact alternative to traditional bulk and fiber-optic systems. Its origin traces back to 1966, when Charles K. Kao proposed that light could be guided through dielectric fibers—a concept that revolutionized telecommunications and laid the groundwork for modern optical communication networks. Decades later, advances in nanofabrication technologies have made it possible to replicate and enhance the functionality of fiber-based and free-space optical systems within a single photonic integrated circuit (PIC).

Much like how electronic integrated circuits (ICs) route and process electrical signals, PICs control and process optical signals using a variety of miniature components. These chips are typically fabricated using CMOS-compatible processes such as deep ultraviolet (DUV) lithography, allowing for high-volume manufacturing and seamless integration with existing electronic platforms. Depending on the application, PICs can be built on diverse material platforms including silicon (Si), silicon nitride (SiN), and indium phosphide (InP), each offering unique benefits in terms of optical confinement, loss, and wavelength compatibility.

A typical PIC integrates a wide range of optical components: waveguides to direct light, couplers to split or combine signals, resonators for filtering or sensing, and active elements like lasers, modulators, and photodetectors for light generation, modulation, and detection. This high level of integration enables the development of compact, energy-efficient, and high-bandwidth systems for applications in telecommunications, data centers, sensing, and emerging quantum technologies.

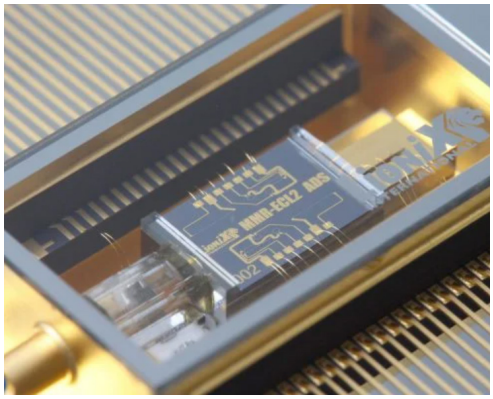

1.2 Underlying Driving force — Rapid Growth of Data Traffic

The explosive growth of global internet traffic has become a defining trend of the digital age. This surge is fueled by a combination of emerging technologies and evolving user demands—including the widespread adoption of mobile internet, the proliferation of high-definition video streaming and real-time communication platforms, the rapid development of artificial intelligence (AI) and edge computing, and the ever-expanding ecosystem of cloud services and Internet of Things (IoT) devices. As data generation and consumption increase at an unprecedented rate, the infrastructure responsible for transporting, processing, and storing this information—particularly data centers—is under immense pressure to scale both capacity and efficiency.

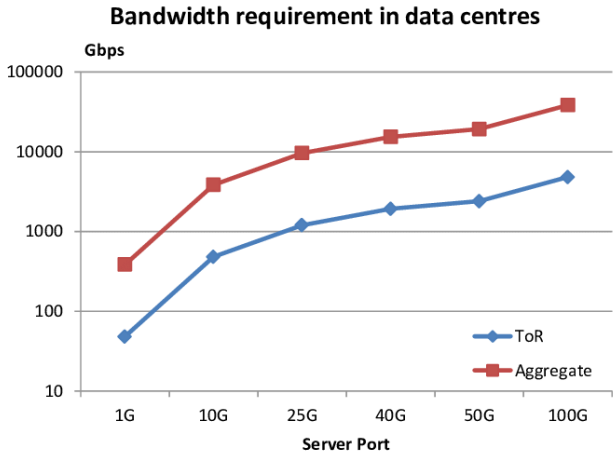

To keep pace with this data-driven demand, next-generation data center interconnects must meet increasingly stringent performance metrics. These include:

- Ultra-high bandwidths exceeding 1 Tbps/link, to accommodate massive volumes of parallel data streams.
- Ultra-low communication latencies below 1μs, essential for real-time applications such as financial trading, online gaming, and AI inference.

- Energy efficiency targets below 1 pJ/bit, a critical requirement for managing the operational costs and environmental impact of large-scale data center operations.

These aggressive performance goals have motivated a global push toward photonic technologies, which offer fundamental advantages over conventional electronic systems in terms of bandwidth and power efficiency. Integrated photonics, in particular, have emerged as a promising solution to address these challenges by enabling high-bandwidth, low-latency optical interconnects within compact and energy-efficient platforms.

1.3 Electrical vs Optical Interconnects in Data Centers

Traditionally, data centers have depended on electrical interconnects—such as copper cables and electronic chips—to transmit data between servers and network components. However, as data rates continue to climb, these electrical solutions encounter significant physical limitations. For example, electrical signals suffer from RC delay, a fundamental issue caused by resistance (R) and capacitance (C) in wires and circuits, slowing down signal transmission. Additionally, the skin effect restricts high-frequency electrical signals to the surface of copper conductors, increasing signal loss and limiting available bandwidth. High-speed electrical interconnects also consume substantial amounts of power, generating heat that demands complex and costly thermal management solutions. Furthermore, electrical systems are inherently susceptible to electromagnetic interference (EMI), which can degrade signal integrity and limit reliability.

In contrast, optical interconnects address these limitations effectively. Optical systems provide substantially greater bandwidth by leveraging advanced multiplexing technologies, such as wavelength-division multiplexing (WDM), enabling many data channels to coexist simultaneously within a single fiber or waveguide. This dramatically increases the data-carrying capacity. Moreover, optical links consume significantly less power, especially over longer distances, because light signals encounter minimal transmission losses and require fewer repeaters or amplifiers. Optical interconnects also offer extremely low latency, making them ideal for applications demanding rapid data processing and real-time responsiveness. Additionally, unlike electrical connections, optical signals are immune to EMI, ensuring more robust and reliable data transmission in densely populated data-center environments.

Given these distinct advantages, optical interconnect technology is increasingly becoming the standard for modern data centers, enabling greater scalability, higher efficiency, and improved system performance.

2. Fundamentals of Integrated Photonics

2.1 Integrated Photonics for Optical Interconnect/Switching

Integrated photonic switches play a crucial role in enabling the next generation of optical interconnects and switching technologies. These devices utilize integrated photonics to achieve compact, scalable, and energy-efficient solutions for optical signal routing within data centers and high-performance computing (HPC) systems. By integrating essential components such as waveguides, modulators, couplers, and detectors onto a single photonic chip, integrated optical switches facilitate ultra-high-throughput and low-latency communication, making them particularly advantageous for demanding applications like artificial intelligence (AI) and machine learning workloads.

The inherent scalability and efficiency of integrated photonic switches significantly reduce the complexity, footprint, and power consumption compared to conventional electrical switching methods. As a result, this technology is increasingly being adopted by major technology companies—including Google, Meta, Amazon, Microsoft, Alibaba Cloud, and others—to address their rapidly expanding data transmission and processing requirements. Leveraging integrated photonics, these companies can build more powerful and energy-efficient data centers, supporting future advancements in AI-driven platforms, cloud computing infrastructures, and large-scale internet services.

2.2 Broad Application Perspectives of Integrated Photonics

Integrated photonics technology is positioned at the intersection of multiple cutting-edge fields, enabling transformative advancements across diverse applications. Its versatile capabilities in handling and processing optical signals open numerous opportunities in optical interconnects, sensing, and computing.

Optical Interconnect Applications:

- Data centers and supercomputers
- Optical I/O and all-optical transmission

- Chip-to-chip optical communication
- 5G/6G fronthaul optical networks
- All-optical metro and access networks

Optical Sensing Applications:

- Integrated spectroemter for biomedical, indusctral spectrosopic applications
- Portable/wearable sensing devices
- Hyperspectral imaging
- Optical coherence tomography (OCT)

Optical Computing Applications:

- AI acceleration photonic chips
- 5G/6G BBU signal processing
- Quantum computing processors
- Linear optical computing chips
- Reconfigurable photonic processors

2.3 Advances in Photonic Integration Technologies

In recent decades, integrated photonics has experienced rapid technological progress, transitioning from simple chip-scale demonstrations to highly sophisticated systems approaching the complexity of electronic very-large-scale integration (VLSI). Key trends, market growth indicators, and persistent technological challenges shape the current landscape of photonic integration.

2.3.1 Emerging Technology Trends:

- Photonic integrated circuits (PICs) have significantly evolved from containing merely a handful of optical components per chip in the early 1990s to exceeding 10^5 components per chip today. This exponential growth now parallels the complexity levels of electronic integrated circuits, enabling unprecedented on-chip optical functionalities.

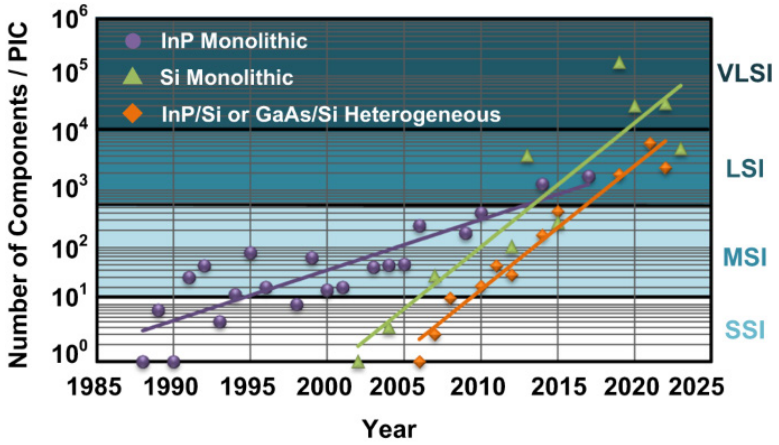

- The industry has moved beyond traditional monolithic integration methods toward heterogeneous integration platforms. This approach seamlessly integrates multiple material systems—such as silicon (Si), silicon nitride (SiN), and indium phosphide (InP)—onto a single photonic chip through advanced wafer-scale processing techniques. Heterogeneous integration allows designers to leverage the strengths of each material, enabling highly optimized and multifunctional photonic chips.
- Modern photonic integration extensively employs CMOS compatible fabrication methods, particularly DUV lithography at the 193 nm wavelength. Combined with wafer-level packaging, these manufacturing techniques facilitate large-scale production, cost-effectiveness, and compatibility with existing electronic fabrication infrastructure.

2.3.2 Market Growth and Industry Adoption:

The photonic integration market has witnessed robust year-over-year growth, driven primarily by the expanding optical transceiver segment. Silicon photonics and InP-based integrated platforms currently dominate this market due to their scalability, performance, and compatibility with high-volume manufacturing. As global data traffic continues to surge, market demand for integrated photonics solutions is expected to further accelerate.

2.3.3 Current Challenges and Barriers:

Despite significant advancements, several technological and market-related challenges remain:

- Unlike the electronics industry, which has long benefited from a universally accepted scaling paradigm known as “Moore’s Law,” integrated photonics currently lacks standardized frameworks or design rules. This absence hampers systematic scalability, interoperability between vendors, and slows widespread adoption.
- A critical bottleneck for silicon-based platforms is the integration of cost-effective, efficient, and reliable on-chip laser sources. Silicon itself does not emit light efficiently, necessitating heterogeneous integration of III-V materials (e.g., InP-based lasers) or external lasers, which adds complexity and cost.
- Achieving precise alignment between optical waveguides and electronic interfaces remains technically challenging. Misalignment even at the sub-micron level can dramatically affect device performance, reliability, and manufacturing yield, necessitating advanced packaging and alignment technologies.

2.4 Fabrication Processes of Integrated Photonic Chips

Fabricating PICs involves precise semiconductor processing techniques to create optical structures at sub-micrometer (or even nanometer) scales. Here, we illustrate the typical fabrication process using a **passive Silicon-on-Insulator (SOI) platform**, which is widely adopted due to its high optical confinement, CMOS compatibility, and excellent manufacturability.

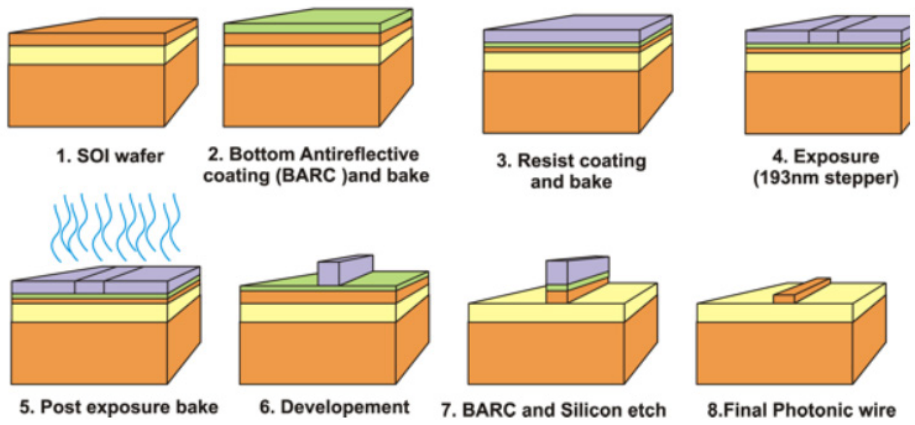

A SOI wafer typically consists of three distinct layers, each serving a specific purpose in the photonic device:

- Top silicon layer (220 nm) serves as the core material for optical waveguides, enabling strong confinement and efficient propagation of optical signals at telecom wavelengths.
- Buried oxide (BOX) layer (2 μm SiO_2) isolates optical signals from the underlying substrate, providing optical confinement and minimizing substrate losses.
- Bottom silicon substrate provides mechanical support for the wafer and assists in heat dissipation during operation.

To define the complex optical structures on the SOI wafer, advanced photolithography and precise etching steps are employed:

- Photoresist coating: The wafer is spin-coated with a thin layer of photosensitive polymer (photoresist), followed by the application of an anti-reflective coating (ARC) to ensure high-resolution pattern transfer.
- Pattern transfer via DUV lithography: The desired waveguide patterns are transferred onto the wafer using DUV lithography (typically 193 nm wavelength), enabling high-resolution features down to tens of nanometers.
- Development and reactive ion etching (RIE): After exposure, the resist patterns are developed chemically, leaving defined areas of silicon exposed. These exposed areas are then etched using RIE, accurately

transferring the patterns into the silicon layer to create waveguides, couplers, resonators, and other components.

Following lithography and etching, the fabricated PIC undergoes additional processing and packaging steps to enhance its functionality, reliability, and integration capability:

- Cladding deposition: An upper protective cladding—commonly SiO_2 or polymer—is deposited over the optical structures to protect them mechanically, provide environmental stability, and optimize optical properties.
- Electrical control and interfacing: Metal pads and electrodes, such as electrothermal heaters, are integrated onto the chip to enable active control and tuning of photonic elements.
- Chip dicing and optical Interfaces: Finally, the fabricated wafers are diced into individual chips. Optical interfaces—either polished edge facets or grating couplers—are precisely fabricated to efficiently couple light between optical fibers and waveguides on the photonic chip.

3. Derivation of Optical Waveguide Modes

3.1 Integrated Optical Waveguide

The integrated optical waveguide is the most fundamental building block of integrated photonic circuits. Similar to how optical fibers guide light over long distances, integrated optical waveguides confine and direct light on a chip-scale platform. They enable precise control of li ght propagation, which is essential for signal transmission, modulation, switching, and other photonic functions.

There are several common types of waveguide structures, classified based on their refractive index profile and confinement geometry:

- **Slab (Planar) Waveguide**: Provides light confinement in only one dimension—typically the vertical direction. It consists of a high-index core layer sandwiched between two lower-index cladding layers. This structure supports propagation along the plane but does not confine light laterally.
- **Strip / Ridge / Wire (Rectangular) Waveguide**: Offers confinement in both vertical and horizontal directions. These are the most widely used waveguides in integrated photonics. The high-index core, usually rectangular in cross-section, is surrounded by lower-index cladding material, allowing strong confinement and tight bending radii.

- **Rib, Slot, and Other Advanced Waveguides**: These waveguides feature more complex geometries to tailor optical field distribution.
    - Rib waveguides combine slab and ridge features to balance mode confinement and fabrication tolerance.
    - Slot waveguides confine light in a low-index gap between two high-index regions, achieving strong field enhancement in the slot region—useful for sensing and nonlinear optics.

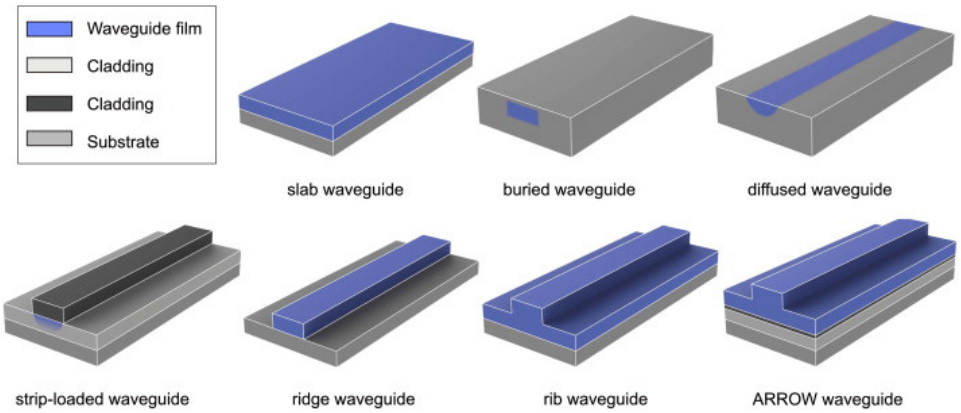

A **waveguide mode** refers to the stable **spatial distribution of the optical field supported by the waveguide**. Each mode represents a specific electromagnetic field pattern, determined by the waveguide geometry and refractive index contrast. In most integrated photonic systems, only the fundamental mode is used to ensure single-mode operation and minimize dispersion or crosstalk.

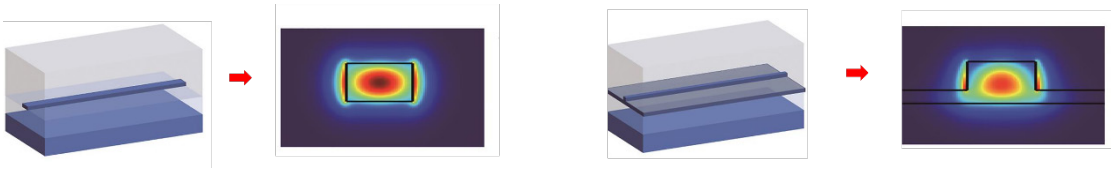

3.2. Fundamentals of Electromagnetic waves

The behaviour of light—as an electromagnetic wave—is fundamentally governed by Maxwell's equations, which describe how electric fields (E, D) and magnetic fields (H, B) are generated and interact with each other and with matter. These equations provide the theoretical foundation for understanding optical wave propagation, light–matter interaction, and mode formation in waveguides.

To analyse wave propagation in optical systems, we typically consider monochromatic waves, i.e., fields oscillating at a single angular frequency ω. Under this assumption, the time-harmonic electric and magnetic fields can be expressed as:

$$\mathbf{E}(r,t) = \mathbf{E}(r)e^{i\omega t}, \mathbf{H}(r,t) = \mathbf{H}(r)e^{i\omega t}$$

Substituting these into Maxwell's equations leads to the Helmholtz wave equations:

$$\nabla^2\mathbf{E}(r) + k^2n^2(r)\mathbf{E}(r) = 0$$
$$\nabla^2\mathbf{H}(r) + k^2n^2(r)\mathbf{H}(r) = 0$$

where k is the free-space wave number, and $n(r)$ is the position-dependent refractive index.

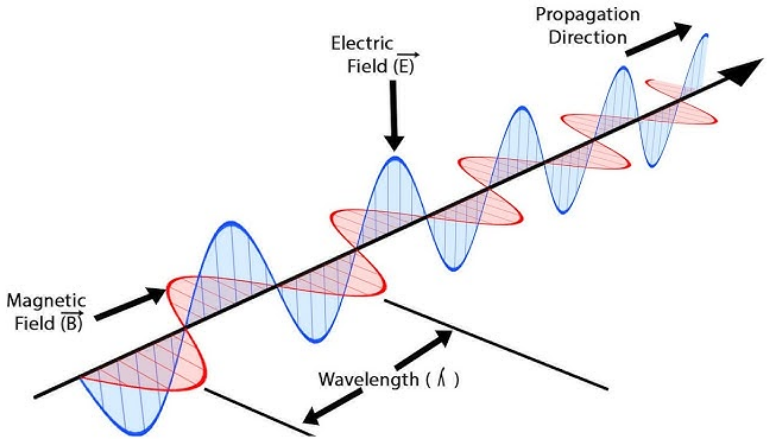

In a uniform medium such as free space, the solution to these equations yields transverse electromagnetic (TEM) waves, in which the electric field $\mathbf{E}$ and magnetic field $\mathbf{H}$ are both perpendicular to the direction of wave propagation and to each other.

3.3. Waveguide modes in a Planar Waveguide

A typical three-layer planar waveguide consists of a high-index core layer (thickness t_g) sandwiched between two lower-index cladding layers. The refractive index varies only in the x-direction, while the waveguide is uniform in the y-direction. We assume wave propagation along the z-direction. Due to the index contrast in the x-direction, true transverse electromagnetic (TEM) modes cannot be supported. Instead, the waveguide supports either TE (transverse electric) or TM (transverse magnetic) modes.

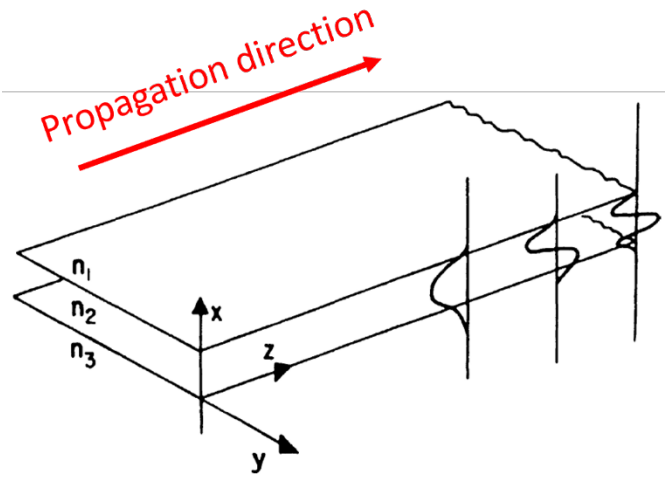

To derive the optical modes in such waveguide, we begin with the Helmholtz equation:

$$\nabla^2\mathbf{E}(r) + k^2n^2(r)\mathbf{E}(r) = 0 \tag{1.1}$$

where $\mathbf{E}(r)$ is the electric field vector, r is the position vector, i.e. $\boldsymbol{r}(x, y, z)$, $n(r)$ is the index of refraction, and $k \equiv \omega/c$ is the free-space wavenumber.

For TE modes, the electric field has only the $E_y$component (i.e., $E_z = 0$). Under the monochromatic assumption, the field can be written as:

$$\boldsymbol{E}(\boldsymbol{r}) = \boldsymbol{E}(x, y)exp(-i\beta z) \tag{1.2}$$

here β is the propagation constant, $\beta = kn_{eff} = \omega n_{eff}/c$.

Substituting Eq. (1.2) into Eq. (1.1) gives:

$$\frac{\partial^2\mathrm{E}(x,y)}{\partial x^2} + [k^2n^2(\mathrm{r}) - \beta^2]\mathrm{E}(x, y) = 0 \tag{1.3}$$

Given the waveguide is uniform in the y-direction, we solve this second-order differential equation separately in each of the three x-regions (core and two claddings):

$$\begin{aligned} \partial^2E(x,y)/\partial x^2 + [k^2n_1^2 - \beta^2]E(x, y) = 0 \\ \partial^2E(x,y)/\partial x^2 + [k^2n_2^2 - \beta^2]E(x, y) = 0 \\ \partial^2E(x,y)/\partial x^2 + [k^2n_3^2 - \beta^2]E(x, y) = 0 \end{aligned} \tag{1.4}$$

The solutions to these equations are either sinusoidal (in the core) or exponential (in the cladding), depending on whether $(k^2{n^2}_i - \beta^2), i = 1,2,3$ is greater than or less than zero. The general solution for $E_y(x)$ is:

$$E_y(x) = \begin{cases} A\exp(-qx) & 0 \le x \le \infty \\ B\cos(hx) + C\sin(hx) & -t_g \le x \le 0 \\ D\exp\left[p\left(x + t_g\right)\right] & -\infty \le x \le -t_g \end{cases} \tag{1.5}$$

Constants $\mathrm{A}, \mathrm{B}, \mathrm{C}, D, q, h,$ and p are determined using boundary conditions, which require the tangential components of both electric and magnetic fields to be continuous across boundaries (i.e., both $E_y(x)$ and $\partial E_y(x)/\partial x$ must be continuous at $x = 0$, and $x = -t_g$).

This yields a normalized form for $E_y(x)$ expressed using a single coefficient C':

$$E_y(x) = \begin{cases} C' \exp(-qx) & 0 \le x \le \infty \\ C' \left[\cos(hx) - \left(\frac{q}{h}\right)\sin(hx)\right] & -t_g \le x \le 0 \\ C' \left[\cos(ht_g) + \left(\frac{q}{h}\right)\sin(ht_g)\right]\exp[p(x + t_g)] & -\infty \le x \le -t_g \end{cases} \quad (1.6)$$

with:

$$\begin{aligned} q &= (\beta^2 - n_1^2 k^2)^{\frac{1}{2}} \\ h &= (n_2^2 k^2 - \beta^2)^{\frac{1}{2}} \\ p &= (\beta^2 - n_3^2 k^2)^{\frac{1}{2}} \end{aligned} \quad (1.7)$$

As $\partial E_y(x)/\partial x$ must be continuous at $x = -t_g$, then:

$$-h\sin(-ht_g) - h(q/h)\cos(-ht_g) = p[\cos(ht_g) + (q/h)\sin(ht_g)]$$

or

$$\tan(ht_g) = \frac{p + q}{h\left(1 - \frac{pq}{h^2}\right)} \quad (1.8)$$

This leads to discrete values of $\beta \Rightarrow \beta_m$ (q_m, h_m and p_m), and the solutions for β_m can be obtained graphically or computed numerically using software tools.

The resulting TE mode profile is characterized by a sinusoidal oscillation of the optical field within the core region (where the refractive index is highest), and an exponential decay of the field in the surrounding cladding regions, forming what is known as the evanescent field or evanescent tail. The number of field nodes in the core determines the mode order. The TE_0 mode, which has no internal nodes, is referred to as the fundamental mode. Higher-order modes, such as TE_1, TE_2, and TE_3, exhibit one, two, three, or more nodes, respectively.

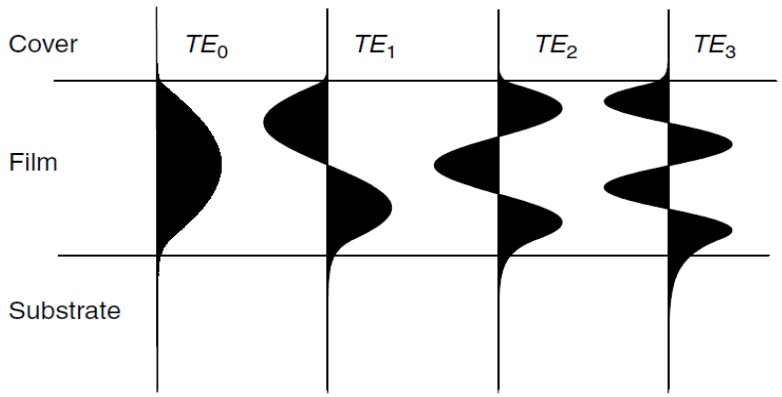

In analog, for TM modes (i.e., $H_z = 0$), we have the fields:

$$H_y(x,z,t) = H_y(x)e^{i(\omega t-\beta z)}$$

$$E_x(x,z,t) = \frac{i}{\omega\varepsilon}\frac{\partial H_y}{\partial z} = \frac{\beta}{\omega\varepsilon}H_y(x)e^{i(\omega t-\beta z)}$$

$$E_z(x,z,t) = -\frac{i}{\omega\varepsilon}\frac{\partial H_y}{\partial x}$$

These equations yield:

$$H_y(x) = \begin{cases} -C'\left[\frac{h}{\bar{q}}\cos\left(ht_g\right) + \sin\left(ht_g\right)\right]\exp\left[p\left(x+t_g\right)\right] & -\infty \le x \le -t_g \\ C'\left[-\frac{h}{\bar{q}}\cos\left(hx\right) + \sin\left(hx\right)\right] & -t_g \le x \le 0 \\ C' - \frac{h}{\bar{q}}\exp\left(-qx\right) & 0 \le x \le \infty \end{cases}$$

Applying boundary conditions ($\partial H_y/\partial x$ is continuous at the n_2-n_3 boundary) leads to:

$$\tan\left(ht_g\right) = \frac{h(\bar{p}+\bar{q})}{h^2-\bar{p}\bar{q}}$$

To summarize, TE modes have the non-zero field components E_y, H_x, and H_z (minor), while TM modes have H_y, E_x and E_z (minor).

3.4. Cutoff Condition for Planar Waveguides

The cutoff condition defines the point at which the optical field transitions from evanescent to oscillatory in the cladding regions (Regions 1 and 3). At this threshold, the mode can no longer be well confined within the waveguide, meaning it becomes unguided.

For symmetrical planar waveguide (i.e. $n_1 = n_3$), at cutoff, β reaches its minimum allowable value, given by:

$$\beta = kn_1 = kn_3$$

Substituting this into the definitions in Eq. (1.7), we find:

$$p = q = 0, h = k(n_2^2 - n_1^2)^{1/2} = k(n_2^2 - n_3^2)^{1/2}$$

To ensure waveguiding of a given mode to occur, one must have (see Eq. 1.8):

$$tan(ht_g) = \frac{p+q}{h(1-pq/h^2)} = 0$$

which requires

$$ht_g = m_s\pi,\ m_s = 0,1,2,3,\ldots$$

From this, we can derive the cutoff condition:

$$\Delta n = (n_2 - n_1) > \frac{m_s^2\lambda_0^2}{4t_g^2(n_2 + n_1)},\quad m_s = 0,1,2,3,\ldots \tag{1.9}$$

This inequality determines which modes can be supported by a waveguide with a given Δn and ratio of λ_0/t_g.

For the fundamental mode ($m_s = 0$)

- $\Delta n > 0 \Rightarrow$ any wavelength could be guided in this mode
- small Δn and/or large $\lambda_0/t_g \Rightarrow$ poor confinement $\Rightarrow$ large evanescent tails.

For an asymmetrical planar waveguide (e.g., $n_2 > n_3 \gg n_1$) , the cutoff condition becomes:

$$\Delta n = (n_2 - n_3) > \frac{(2m_a+1)\lambda_0^2}{16(n_2+n_3)t_g^2} = \frac{m_s^2\lambda_0^2}{4(n_2+n_3)\left(2t_g\right)^2} \tag{1.10}$$

where

$$m_s = (2m_a + 1), m_a = 0,1,2,3,\ldots$$

This form shows that only odd-order modes (with odd m_s) are supported in the asymmetric waveguide, and that they are similar to the modes of a symmetric waveguide with twice the core thickness.

3.5. Waveguide modes in a Strip (rectangular) Waveguide

To simplify the analysis of rectangular waveguides, we adopt Marcatili's method—an approximate analytical approach that assumes all modes are well-guided, i.e., operating above the cutoff condition.

In this approximation:

- The field magnitudes in the corner regions (where two boundaries meet) are assumed to be negligible and can be ignored.
- The field decays exponentially in Regions 2–5, with the majority of the optical power confined to Region 1 (the core).

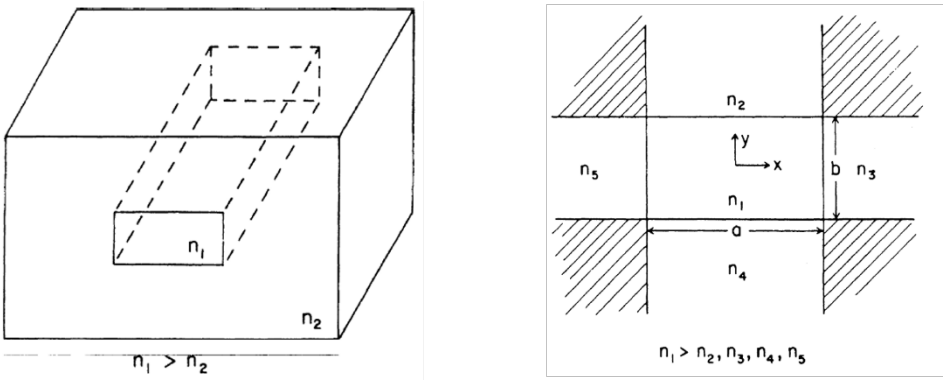

Since the index contrast exists in both the *x* and *y* directions, the electric field can be denoted as E_{pq}^{x} and E_{pq}^{y}, i.e. the electric field distributing along either x or y direction. Here p and q represent the number of field peaks (nodes) in the *x* and *y* directions, respectively. For E_{pq}^{x} modes, the dominate field components are E_x and H_y, whereas for E_{pq}^{y} modes, the dominate components are E_y and H_x.

For example, the mode profile of E_{00}^{y} is as follows:

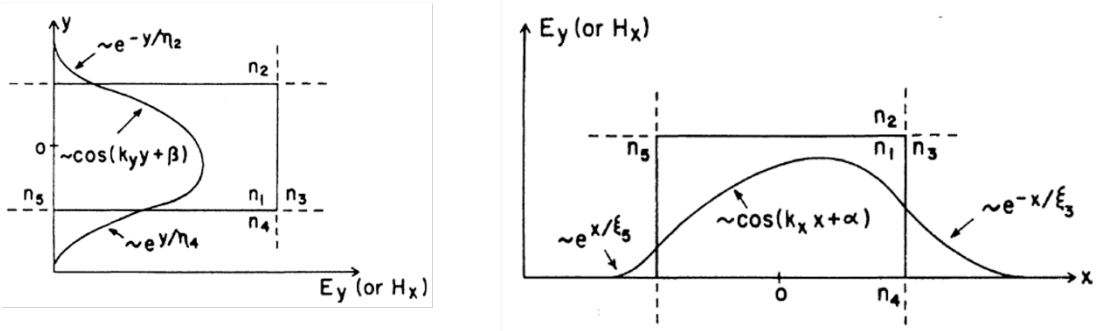

Note that the shape of the mode is characterized by extinction coefficients η_2, ξ_3, η_4, and ξ_5 in the regions where it is exponential, and by propagation constants $\mathrm{k_x}$ and $\mathrm{k_y}$ in Region 1.

In practice, the width (*x*-direction) of a rectangular waveguide is usually larger than its height (*y*-direction), for example, a 500 nm × 220 nm SOI waveguide. In such cases:

- The refractive index contrast along y-direction is stronger, leading to tighter confinement and typically a single-peaked field profile without nodes (i.e., no oscillations along *y*).

- Along x-direction, the confinement is weaker, making it easier to form higher-order modes with multiple nodes/peaks.

Thus, the dominant field profiles are usually of the form E_{pq}^{y} ($p = 0,1,2,3, \ldots$ and $q = 0$), and the supported modes are known as **quasi-TE modes.**

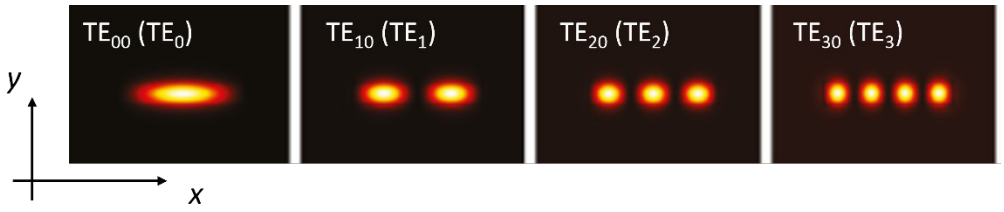

4. Coupling Between Waveguides

When two waveguides are brought close to each other, a phenomenon called mode coupling occurs, which means that optical energy periodically transfers between the two waveguides.

This happens because:

- The evanescent fields of the two waveguides extend into the surrounding space, and when placed close enough, they overlap and interact.
- This interaction enables periodic energy transfer between the two waveguides, where energy oscillates back and forth between the waveguides (like beating)

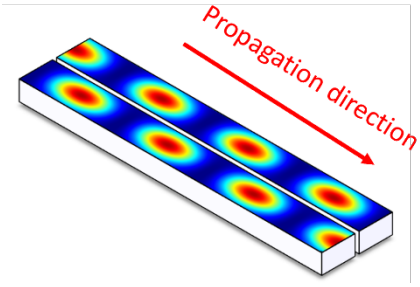

Coupling between two identical lossless waveguides ($\beta = \beta_0 = \beta_1$), and the field of the propagating mode is denoted, as:

$$\bar{E}(x, y, z) = A(z)\bar{\mathcal{E}}(x, y)$$

where $A(z)$ is the complex amplitude of the field, such that the mode power equals

$$P(z) = |A(z)|^2 = A(z)A^*(z)$$

The mode coupling can be described by the general coupled mode equations for the amplitudes of the two modes:

$$\begin{cases} \dfrac{dA_0(z)}{dz} = -i\beta A_0(z) - i\kappa A_1(z) \\ \dfrac{dA_1(z)}{dz} = -i\beta A_1(z) - i\kappa A_0(z) \end{cases} \tag{1.11}$$

where β_0 and β_1 are the mode propagation constants, and κ is the coupling coefficient between modes, which quantifies the strength of interaction between the two waveguides: the larger κ, the faster the energy transfer between them.

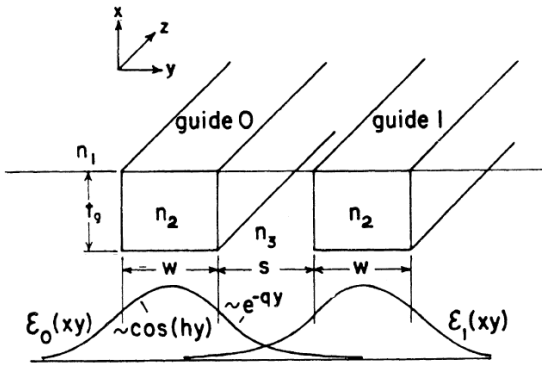

For example, assume that the light is all within Waveguide 0 at the position $z = 0$, i.e.:

$$A_0(0) = 1 \; and \; A_1(0) = 0$$

Thus, the solutions of the coupled mode equations Eq. (1.11) are:

$$\begin{cases} A_0(z) = \cos(\kappa z) e^{-i\beta z} \\ A_1(z) = -i\sin(\kappa z) e^{-i\beta z} \end{cases}$$

And the power flow in waveguides can be expressed as:

$$\begin{cases} P_0(z) = A_0(z) A_0^*(z) = \cos^2(\kappa z) \\ P_1(z) = A_1(z) A_1^*(z) = \sin^2(\kappa z) \end{cases}$$

It can be seen that the coupling length L necessary for complete transfer of power from one waveguide to the other is given by:

$$L = \frac{\pi}{2\kappa} + \frac{m\pi}{\kappa}, m = 0,1,2,3 \ldots$$

5. Simulation Tools for Integrated Photonic Design

Designing and analyzing optical waveguides and integrated photonic components involves solving complex mathematical equations governing the propagation of electromagnetic waves. Due to the intricate nature of these theoretical models,

specialized computer programs and simulation tools have been developed to streamline and facilitate the design, optimization, and validation of photonic structures.

Ansys Lumerical FDTD/MODE

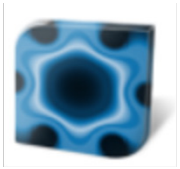

COMSOL Multiphysics (FEM)

Several advanced commercial software packages are widely utilized for optical waveguide mode analysis and device simulation. Notably:

- Ansys Lumerical (FDTD/MODE Solutions): Lumerical is a popular suite of photonic design tools employing Finite-Difference Time-Domain (FDTD) and Eigenmode Expansion (EME) methods. It is particularly effective for modeling wave propagation, analyzing waveguide modes, simulating optical scattering and coupling phenomena, and performing comprehensive photonic component simulations.
- COMSOL Multiphysics (FEM): COMSOL utilizes the Finite Element Method (FEM), enabling the simulation of intricate multiphysics problems, including optical, electrical, thermal, and mechanical interactions within photonic devices. Its powerful and flexible framework is well-suited for in-depth device optimization, complex geometry handling, and integrated multiphysics analysis.

Throughout the upcoming sessions, we will primarily utilize the Ansys Lumerical simulation environment, alongside Matlab-based numerical models. These tools will assist us in performing accurate and efficient calculations, optimizing device structures, and exploring the underlying physical phenomena in optical waveguides and related integrated photonic components.

6. Tasks

Overall, this course includes **three main tasks.** Detailed descriptions can be found in the accompanying ***Task Instructions***:

1. **Waveguide Mode analysis using MATLAB**: Use your own MATLAB scripts to numerically analyse key waveguide mode properties, such as cutoff width and mode order.
2. **Analytical derivation based on the coupled-mode equations**: Solve the coupled-mode equations to understand power exchange between

waveguides and derive expressions for field amplitudes and coupling length.

3. **Mode Coupling Simulation Using Lumerical FDTD:** Simulate mode coupling under different configurations (e.g., varying waveguide spacing, symmetric vs. asymmetric couplers), visualize field evolution, and compare the results with theoretical predictions.

Report Format

Submit your results as **three separate reports**, corresponding to the tasks above:

- **Report 1** (MATLAB-based analysis)
- **Report 2** (Coupled-mode theory derivation)
- **Report 3** (Mode coupling simulation and discussions)

Each report should include key results, figures, and thoughtful analysis.